IEEE Access
Multidisciplinary | Rapid Review | Open Access Journal

Received December 15, 2021, accepted January 4, 2022, date of publication February 7, 2022, date of current version March 4, 2022.

Digital Object Identifier 10.1109/ACCESS.2022.3149801

Adaptive Wide-Area Control of Power Systems Through Dynamic Load Modulating SVCs

AMIN SHARAFI[1], (Graduate Student Member, IEEE), ARASH VAHIDNIA[1], (Senior Member, IEEE), MAHDI JALILI[1], (Senior Member, IEEE), AND GERARD LEDWICH[2], (Life Fellow, IEEE)

[1]School of Engineering, RMIT University, Melbourne, VIC 3000, Australia
[2]School of Electrical Engineering and Computer Science, Queensland University of Technology (QUT), Brisbane, QLD 4000, Australia

Corresponding author: Amin Sharafi (s3201840@student.rmit.edu.au)

ABSTRACT This paper presents an adaptive wide-area control strategy based on energy function. The proposed method enhances the post-fault oscillation damping capability of Static Var Compensators (SVC) by incorporating load dynamics in the wide-area controller design that adapts to load variations. The load dynamics are obtained using Phasor Measurement Units (PMU) through load power and voltage data measurements, which are used to estimate a Moving Average (MA) dynamic load model. The obtained load model is then integrated into the wide-area controller to obtain the required SVC supplementary control action which modulates the load power in response to a disturbance based on inter-area dynamics obtained by employing a nonlinear Kalman filter and PMU measurements. The performance of the proposed strategy is evaluated on the simplified 14 generator model of the southeast Australian power system by using composite load models comprised of induction motor loads of various sizes and combinations. The obtained results show significant improvements in the system stability when the proposed control strategy is applied.

INDEX TERMS Inter-area oscillations, wide-area-control, energy function, FACTS devices, phasor measurement unit, load modeling.

I. INTRODUCTION

Inter-Area oscillations are one of the most critical challenges in design and operation of interconnected power systems. These oscillations can have a detrimental effect on stability and performance, and if not appropriately addressed, they may destabilize and deteriorate the system [1], [2]. The growing demand for electricity and lack of new generation and transmission infrastructure due to the cost and environmental factors as well as the introduction of renewable energy sources have made power systems more stressed and susceptible to low-frequency inter-area oscillations, which are often poorly damped [3], [4].

To address inter-area oscillations and their adverse effects on stability, researchers have developed many control methods that have relied on the utilization of Flexible AC Transmission Systems (FACTS). Traditionally, damping control strategies based on local measurements have been developed by utilizing FACTS, such as Controlled Series Devices (CSD) and Static Var Compensator (SVC) [5]–[7]. Localized control strategies can generally display poor damping performance due to the low observability of inter-area oscillations through local measurements [8], [9]. The limitations imposed by local measurements can be overcome using wide-area control and measurement systems and wide deployment of Phasor Measurement Unit (PMU) devices [10], [11]. This has provided a framework for development of centralized wide-area control strategies. A number of methods have been proposed in the literature based on decentralized and hierarchical approach, model-based and indirect adaptive power oscillation damping, nonlinear control based on reducing affine scheme, robust coordination approach, state feedback and model predictive control (MPC), gravitational search algorithm (GSA) based dual proportional integral (DPI) and bat-inspired algorithm (BIA) based MPC load frequency control (LFC) [12]–[17].

Some of the existing methods are based on the Lyapunov energy function, which is widely used in stability assessment and power systems control [18]–[27]. In designing control algorithms based on energy function, various control signals,

The associate editor coordinating the review of this manuscript and approving it for publication was Salvatore Favuzza.

such as generator rotor angle, frequency deviation, tie-line active and reactive power have been used [18]. In the existing literature, load power deviation has been chosen as the control signal in many SVC based strategies since SVCs have been utilized in load and power flow control applications [18], [21]–[23]. This paper presents such a method, where the load active power deviation is used as the control signal to formulate the SVC based wide-area control algorithms. However, in this paper, the energy function-based wide-area control algorithms are formulated by integrating load dynamic characteristics in the controller design and adapting to load variations to enhance the damping of post-fault low-frequency inter-area oscillations. Load dynamic characteristics are modeled as a Moving Average (MA) process by obtaining load dynamic characteristics by using PMU measurements. The approach in [28] has demonstrated that load dynamics can be estimated and represented as a mathematical model obtained through the application of SVC and PMU devices, which is applicable to any power system equipped with wide-area measurement systems and FACTS devices. This approach has been adopted and modified in this paper to suit the application on hand.

Given the vast number of system dynamic states, the targeted estimation of inter-area dynamics for wide-area control is crucial since the full state control of system generators due to the large computational load is deemed impractical [23], [29]. On this basis, it is more practical to develop wide-area control algorithms based on a reduced system model that targets inter-area dynamic states that affect system stability. The method proposed in [30] demonstrates such an approach where a reduced aggregated system model representative of inter-area dynamics is developed by using a limited number of PMUs and a nonlinear Kalman filtering approach, which is also adopted and applied in this paper.

The performance of the proposed wide-area control approach is evaluated on the simplified 14 generator model of the Southeast Australian power system and simulations are carried out by using a commercial power system simulation software package (DIgSILENT Power Factory). In the performed simulations, a composite load model that consists of small and large induction motor loads is chosen to add complex dynamics to the system, which is further diversified by including induction motor loads of varying sizes and combinations. The obtained results show the feasibility of the proposed wide-area control strategy and its effectiveness in suppressing post-fault low-frequency inter-area oscillations.

In summary, the contributions of this paper are as follows:

- Present a new energy function based wide-area control strategy to damp post-fault low-frequency inter-area oscillations by using SVCs
- The oscillation damping capability of SVCs are enhanced by integrating load dynamic in the design of the wide-area controller
- Load dynamics are modeled and integrated into the wide-area controller as moving average (MA) models by using SVCs and PMUs
- The proposed wide-area control strategy is applied on the simplified 14 generator model of the Southeast Australian power system using a composite load model consisting of various combinations of induction motor loads to add complex dynamics to the system and proven to be feasible

The paper is organized as follows: Section II describes the Energy Function-based wide-area control method and estimation of inter-area dynamics by using PMU measurements and the nonlinear Kalman filtering approach. In section III, the estimation of load dynamics for wide-area control is presented. In section IV, the implementation of the wide-area control method is described and in section V, the wide-area control method is applied to the test system through simulation. The conclusion is given in section VI.

II. WIDE-AREA CONTROL OF INTER-AREA OSCILLATIONS BASED ON ENERGY FUNCTION

Lyapunov energy function has been widely used in stability assessment and control of power systems. Based on the Lyapunov theorem, the stability of a power system can be assessed by examining the transient energy of the system at the instant of fault clearing, which is responsible for the swing of synchronous generators away from the equilibrium point of operation. During a transient event, the transient energy of the post-fault system is converted to kinetic energy, which must be absorbed by the system for its stability to be maintained [21], [24], [25]. In order to enhance the stability of a power system, the reduction rate of kinetic energy has to be increased as much as possible to accelerate the absorption rate of kinetic energy by the system. This objective is achieved through kinetic energy-based control by maximizing the reduction rate of kinetic energy, which brings the system back towards stability [25], [26]. Considering a power system with n coherent generator groups (areas), the dynamics of the system based on the classical aggregate machine model can be expressed as:

$$M_i\ddot{\delta}_i = P_{mi} - P_{li} - P_{ij} - D_i\dot{\delta}_i \qquad \mathrm{i} = 1, 2, 3, \ldots, n \tag{1}$$

where M_i is the inertia, δ_i is the area angle, P_{mi} is the area mechanical power, P_{li} is the area load, P_{ij} is the power transferred between areas and D_i is the damping factor. The absorbed kinetic energy is treated as excess energy that needs to be dissipated by the system for its stability to be preserved. In practice, this can be performed by increasing area loading, which results in dissipation of the absorbed excess energy by area loads. Kinetic energy-based control formulation is useful in this regard since kinetic energy can be expressed in terms of area load power. Given the classical aggregate machine model, the kinetic energy-based control can be formulated as follows:

$$V_{KE} = \frac{1}{2}\sum_{i=1}^{n} M_i\dot{\delta}_i^2 \tag{2}$$

$$\dot{V}_{KE} = \sum_{i=1}^{n} M_i \dot{\delta}_i \ddot{\delta}_i \tag{3}$$

$$\dot{V}_{KE} = \sum_{i=1}^{n} \left(P_{mi} - P_{li} - P_{ij} - D_i \dot{\delta}_i\right) \dot{\delta}_i \tag{4}$$

$$\frac{\partial \dot{V}_{KE}}{\partial P_{li}} = -\dot{\delta}_i \tag{5}$$

$$\Delta P_{li} = k \dot{\delta}_i \tag{6}$$

Equation (2) represents the total kinetic energy of the system and the derivative of kinetic energy is given in equation (3). By substituting equation (1) in (3), the derivative of kinetic energy can be expressed as a function of area load power as shown in equation (4). The partial derivative of kinetic energy with respect to area load power is shown in equation (5). This means that the objective of maximizing the reduction rate of kinetic energy with respect to change in area load is achieved when change in load power ΔP_{li} is equal to $k\dot{\delta}_i$ as in equation (6) where k is an adjustable gain chosen based on the severity of the required control action.

Given the complexity and large number of system dynamic states, from a practical point of view, the proposed wide-area control approach relies on estimation of a reduced system aggregate model for control formulation and representation of inter-area dynamics and post-fault low-frequency oscillatory modes triggered by a contingency. The estimation of the reduced aggregate system model relies on identifying coherent generator groups to aggregate them into dynamic equivalents, allowing the inter-area dynamics of the system to be represented by a set of simplified equivalent machines and interconnections as described in [31]. The reduced equivalent aggregate model parameters are estimated based on online processing of data acquired by PMUs, which are strategically placed across the system to be more sensitive to inter-area oscillations while being less sensitive to local modes of oscillation. Due to the nonlinear nature of post-fault power systems, the effects of local modes on the estimation of post-fault inter-area dynamics are reduced by employing the nonlinear Kalman filtering approach described in [21], [30]. It estimates the equivalent aggregated system angles and velocities by using a limited number of PMUs, that represent inter-area interactions of the system which can be expressed by a set of nonlinear differential-algebraic equations (DAE):

$$\begin{cases} \dot{\boldsymbol{x}} = f\left(\boldsymbol{x}, \boldsymbol{u}\right) \\ \boldsymbol{y} = \boldsymbol{g}\left(\boldsymbol{x}, \boldsymbol{u}\right) \end{cases} \tag{7}$$

where the state vector $\boldsymbol{x}$ contains angles and velocities of aggregated areas represented by the classical machine model, the vector $\boldsymbol{u}$ contains control inputs, and the output vector $\boldsymbol{y}$ contains PMU measurements. The nonlinear Kalman Filter can be summarized as:

$$\bar{x}_k = f_d\left(\hat{x}_{k-1}, u_{k-1}\right) \tag{8}$$

$$\bar{y}_k = H\bar{x}_k \tag{9}$$

$$\hat{x}_k = f_d\left(\hat{x}_{k-1}, u_{k-1}\right) + L_k\left(y_k - \bar{y}_k\right) \tag{10}$$

where $\bar{x}_k$ and $\hat{x}_k$ are predicted and updated system states, $\bar{y}_k$ is the vector of measurements observed by PMUs, H represents the relationship between the predicted states and PMU measurements, L_k is the Kalman filter gain and f_d is the discretized nonlinear swing equation of the identified reduced aggregated model. By employing the proposed nonlinear Kalman filtering approach, the inter-area dynamics of the system are estimated while the effects of local modes from PMU measurements are significantly reduced.

The proposed wide-area control approach is designed to improve the stability and damping performance of the system by suppressing post-fault inter-area oscillations through combining the kinetic energy-based control and the nonlinear Kalman filtering approach, which relies on a limited number of PMU measurements in order to estimate a reduced system model that only targets inter-area dynamics. The estimations of inter-area dynamics by the nonlinear Kalman filtering approach provide instantaneous estimations of equivalent angles and velocities of the reduced aggregated system model, ensuring the feasibility of real-time application of the proposed wide-area control approach on large scale power systems [23]. The proposed wide-area control method can be applied on controllable devices, such as FACTS which are widely available across many power systems to enhance stability.

III. ESTIMATION OF DYNAMIC LOAD MODELS FOR WIDE-AREA CONTROL OF INTER-AREA OSCILLATIONS

Load models play an important role in power system stability studies. The motivation for load modeling has emerged from the fact that load dynamics significantly affect system stability in terms of voltage, frequency, and modes of oscillation [32]–[35]. The problem of load model development has been approached distinctively by component and measurement-based techniques, where the component-based methods are proven to be impractical in large-scale power systems due to load diversity and lack of prior knowledge of load composition. However, measurement-based techniques remain the most practical solution, given the recent advancements in wide-area measurement systems which are nowadays widely used by power system operators [10], [28], [32].

In power system stability studies, the effects of load dynamics on oscillatory modes have been long realized. It was shown in [28] that variations in the composition of loads could affect oscillatory modes in terms of frequency and intensity, and dynamic load models could be developed through excitation and measurements of load dynamics and system identification methods to estimate a dynamic load model for the detailed representation of load behavior in the range of low-frequency oscillatory modes. Given that such a model could be developed, the adverse effects of load dynamics on oscillatory modes could be addressed by incorporating load dynamics in the wide-area controller design that adapts to load variations for enhanced damping and suppression of oscillatory modes triggered by a contingency. For the proposed wide-area control method, load models are developed

to represent load dynamics in the frequency range of inter-area oscillations (0.1 – 0.8 Hz [1, 2]), which are the targets of the proposed adaptive wide-area control method. This is achieved by excitation of load dynamics and utilizing data processing and filtering techniques to extract load dynamics in the range of inter-area oscillations measured by PMUs located at load buses that capture the aggregated load dynamics at the transmission level.

In the implementation of the proposed wide-area control method, the load dynamics are modeled as a moving average (MA) process since the output state of the MA model can be expressed as a function of present and past or present and predicted future input states regardless of past or predicted future outputs. This model structure is useful for the implementation of the wide-area controllers since the MA load models need to be obtained based on the present and predicted future input states to eliminate possible variations and delays between successive wide-area measurements that can occur between past and present measured input states, which can degrade the performance of wide-area controllers. Therefore, by relying on present and predicted future input states, the possibility of adverse effects of variations and delays between successive wide-area measurements on the performance of wide-area controllers is eliminated since the present and predicted future input state values are obtained at the same instant.

In a wide-area controlled power system, dynamic load models can be developed by employing controllable devices, such as FACTS and PMU measurements. The load dynamics can be excited through small voltage fluctuations imposed by FACTS devices and subsequently measured by PMUs through wide-area measurement and control infrastructure. In this study, the load modeling process is performed by using SVCs as they are widely available across many power networks such as the Australian grid. The proposed wide-area control method and load modeling process are applied on the simplified 14 generator Southeast Australian power system [36] for verification which uses SVCs. In summary, the MA load model can be developed by following the steps outlined below:

1. Excitation of load dynamics by SVC
2. Measurement of load power and voltage data
3. MA load model parameter estimation

The excitation of load dynamics is performed by an SVC, which can inject a low amplitude noise signal in the form of a uniform random number into the SVC's auxiliary control input, which is added to the SVC's reference voltage. This results in small voltage fluctuations in load terminal voltage. Due to the voltage dependency of loads, the resultant voltage variations will result in direct variation in load power. The block diagram of the SVC with noise injection is shown in Figure 1. PMU measurements obtain the response of load power to voltage variations over a specific time window, which is served as the raw data for load modeling. The block diagram of Load, SVC and PMU locations is shown

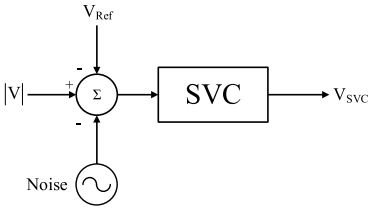

FIGURE 1. SVC block diagram with added noise signal.

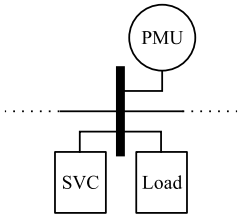

FIGURE 2. Load, SVC and PMU location.

in Figure 2. The development of the MA load model begins by processing the measured load power and voltage data obtained through PMU measurements. This process involves resampling and filtering the measured data to extract inter-area dynamics within the frequency range of 0.1 – 0.8 Hz [1, 2]. A suitable MA model order is then chosen depending on the required input state samples, resulting in an accurate estimation of the output values. The MA model structure is given as:

$$MA\,(m) : y_t = b_0 u_t + b_1 u_{t+1} + b_2 u_{t+2} + b_3 u_{t+3} + \ldots + b_m u_{t+m} \tag{11}$$

where y and u are the input and output, m, t, and b are the order of MA model, sample number, and model coefficients, respectively. The parameters of the MA model can be represented in a more compact form by using vector notation as follows:

$$\beta = [b_0\ b_1\ b_2\ b_3\ \ldots\ b_m]^T \tag{12}$$

$$\varphi = [u_t\ u_{t+1}\ u_{t+2}\ u_{t+3}\ \ldots\ u_{t+m}]^T \tag{13}$$

Therefore, the MA model can be written as:

$$MA\,(m) : y_t = \varphi^T \beta \tag{14}$$

The coefficients β can be estimated by using the least square method, as shown below:

$$\sum_{t=1}^{M} \varphi y_t = \sum_{t=1}^{M} \varphi\varphi^T \beta \tag{15}$$

$$\hat{\beta} = \left[\sum_{t=1}^{M} \varphi\varphi^T\right]^{-1} \sum_{t=1}^{M} \varphi y_t \tag{16}$$

where $\hat{\beta}$ denotes the estimated model coefficients. In order to determine the accuracy of the estimated MA model, the measurement data is compared against the output of the

estimated MA model. This is achieved by calculating the Root Mean Square Error (RMSE) percentage value, which is given as:

$$\%fit = \left(1 - \frac{\|y - \hat{y}\|}{\|y - mean\,(y)\|}\right) \times 100 \tag{17}$$

IV. IMPLEMENTATION OF THE WIDE-AREA CONTROL METHOD

In this section, the implementation of the proposed adaptive wide-area control method is presented. The wide-area controllers are intended to be applied to FACTS devices, such as SVCs, which are often placed near long interconnectors or major load centers due to their good voltage regulation capabilities. The mode of operation and control of SVCs are determined based on their location. The SVCs located at long interconnectors between areas mainly modulate the impedance of the lines between areas, while those located inside areas mainly modulate the area load through direct voltage manipulations due to the voltage dependency of loads [21]. The proposed adaptive wide-area controllers are applied to load modulating SVCs to address the adverse effects of load dynamics on post-fault inter-area oscillations by enhancing SVC load modulating capability through integrating load dynamics in the wide-area controller design and adapting to load dynamics variations.

The implementation of the wide-area control method relies on the nonlinear Kalman filtering approach to estimate the inter-area dynamics of the system in terms of angles and velocities, as described in section II. The load dynamic characteristics are modeled as a moving average (MA) process in the frequency range of inter-area oscillations using SVC and PMU measurements, as described in section III.

The adaptive wide-area control of SVCs is based on the kinetic energy-based control algorithm expressed in equations (2) − (6). The control algorithm calculates the desired change in area load power as a function of area velocity which reduces the excess kinetic energy of the system during a transient event as described in section II. The calculated desired change in area load power by the control algorithm can be directly applied to a load modulating SVC as a supplementary voltage control input due to the relative proportionality between area load power and voltage. On this basis, it is possible to express the change in SVC voltage as a function of change in area load power:

$$\Delta V_{SVC_i} = f(\Delta P_{li}) \tag{18}$$

where ΔP_{li} is the change in area load power and ΔV_{SVC_i} is the change in SVC voltage located at area i. On this premise, the supplementary control of the SVC can be expressed by substituting equation (6) into equation (18) which can be written as:

$$u_i = k\dot{\delta}_i \tag{19}$$

where $\dot{\delta}_i$ is the velocity, k is the control gain and u_i is the supplementary control input of the SVC located at area i. This approach works well; however, the efficacy of this approach tends to diminish when loads with large portions of complex dynamics are considered, which resembles a more realistic scenario. Therefore, the complex dynamics of loads need to be considered to further improve the performance of wide-area controlled load modulating SVCs. For this purpose, the dynamic relationship between the change in area load power and change in SVC voltage is modeled more accurately as a moving average (MA) process and can be expressed as:

$$\begin{aligned}\Delta V_{SVC_{i_t}} &= b_0\Delta P_{li_t} + b_1\Delta P_{li_{t+1}} + b_2\Delta P_{li_{t+2}} \\ &\quad + \ldots + b_m\Delta P_{li_{t+n}}\end{aligned} \tag{20}$$

On this basis, the supplementary control of SVCs can be obtained by substituting equation (6) into equation (20) which expresses the load modulating wide-area SVC control action based on load dynamics which can adapt to load changes by applying the dynamic load modeling process to update the MA load model parameters on regular intervals. Therefore, the adaptive wide-area supplementary control of the SVC can be expressed as:

$$\begin{aligned}u_{i_t} &= b_0 k\dot{\delta}_{i_t} + b_1 k\dot{\delta}_{i_{t+1}} + b_2 k\dot{\delta}_{i_{t+2}} \\ &\quad + \ldots + b_m k\dot{\delta}_{i_{t+n}}\end{aligned} \tag{21}$$

where u_{i_t} is the wide-area supplementary control input of the SVC located at area i at sampling instant t, which is calculated based on the present and future predictions of area velocities $\dot{\delta}_{i_t}, \dot{\delta}_{i_{t+1}}, \dot{\delta}_{i_{t+2}}, \ldots, \dot{\delta}_{i_{t+n}}$ obtained by nonlinear Kalman filter estimations and load dynamics represented by MA model coefficients $b_0, b_1, b_2, \ldots, b_m$. The block diagram representation of the proposed adaptive wide-area controller and the SVC model is shown in Figure 3. The wide-area control signal is fed into the summing point along with the SVC's reference and bus voltage signals as a supplementary control input, which adjusts the SVC's bus voltage according to load dynamics to stabilize the system and damp the post-fault inter-area oscillations triggered by a contingency.

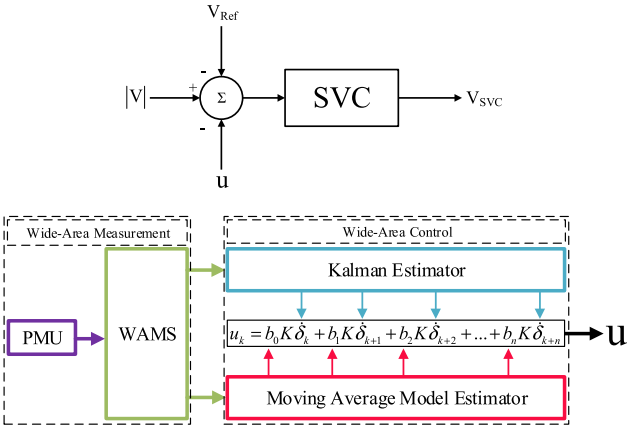

FIGURE 3. SVC and adaptive wide-area controller block diagram.

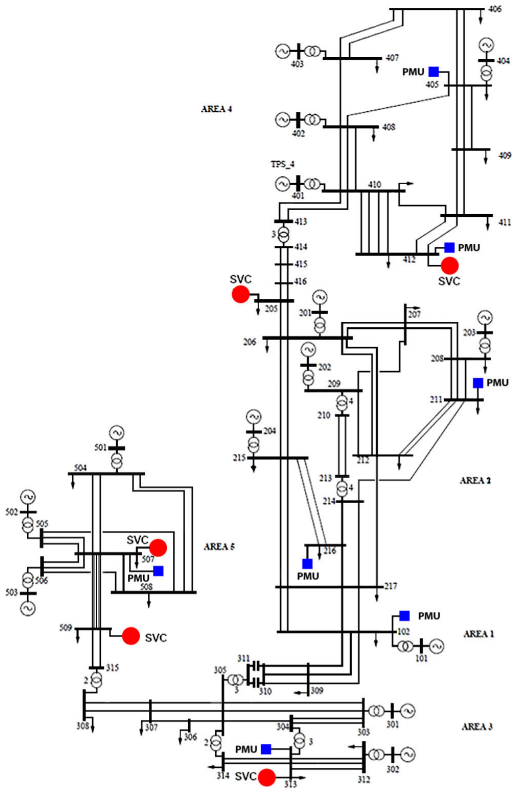

FIGURE 4. Simplified 14 generator southeast australian power system.

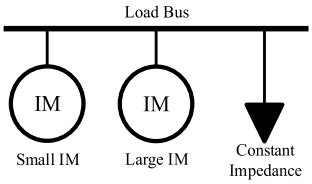

FIGURE 5. Composite load model with induction motor (IM) loads.

V. APPLICATION AND SIMULATION OF THE WIDE-AREA CONTROL METHOD

The performance of the proposed adaptive wide-area control method was evaluated on the simplified 14 generator model of the Southeast Australian power system [36], which is shown in Figure 4. The proposed adaptive wide-area control method was implemented in DIgSILENT Power Factory simulation software package. The presented test system consists of five areas that are based on the Southeast Australian power network. The test system includes several load and line modulating SVCs, as highlighted in Figure 4. The wide-area controllers were applied to load modulating SVCs located at buses 313, 412, and 507, which are close to major loads.

The nonlinear Kalman filtering method proposed in [28] was applied to estimate the equivalent inter-area dynamics of the system in terms of area angles and velocities by using PMUs located at system buses 102, 211, 216, 313, 405, 412 and 507 which are placed based on real PMU locations in the Australian National Grid.

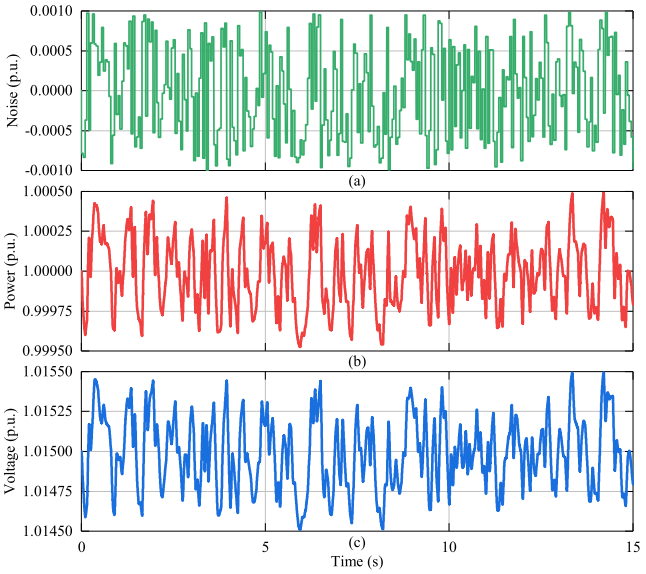

FIGURE 6. An example of (a) uniform random noise, (b) measured load power and (c) measured voltage data by PMU at SVC Bus 313 for 50% dynamic load.

The proposed MA load modeling method was applied to estimate load dynamics in the frequency range of inter-area oscillations, as seen by the load modulating SVCs through excitation of load dynamics and PMU measurements to obtain load power and voltage data. For this purpose, PMUs located at buses 313, 412 and 507 are utilized which directly measure load dynamics observed from load modulating SVC buses. In this study, a low amplitude uniform random noise signal limited in the range of ± 0.001 p.u. was used for excitation of load dynamics by SVCs over a measurement period of 60 seconds which does not impose any adverse effect on the operation and stability of the system. An example of measured load power and voltage data by the PMU located at SVC bus 313 for 15 seconds is shown in Figure 6, which illustrates the load power and voltage fluctuations resulting from uniform random noise injected by the SVC. The adaptive wide-area controllers are then constructed and applied on load modulating SVCs by combining nonlinear Kalman filter estimations of area velocities and MA dynamic load model parameters according to the adaptive wide-area SVC control expression presented in equation (21).

The test system was simulated with several loading conditions which three of them are chosen for demonstration. In the presented cases, the composition of system loads was chosen to comprise a combination of dynamic and static loads in the form of induction motor and constant impedance loads, as shown in Figure 5. This load composition was selected since induction motors constitute a substantial portion of electrical loads with complex dynamics. Combinations and parameters of induction motors used in simulations are presented in Tables 4 and 5 respectively. It is essential to note the significance of including load dynamics in the design of the adaptive wide-area controller as it results in better inter-area oscillations damping through more effective SVC

load modulation. This will be demonstrated in a series of comparisons where the performance of the proposed adaptive wide-area control approach is compared against the wide-area control method presented in [21] where the load modulation is carried out without considering the load dynamics in controller design.

The importance of frequent load modeling and adapting to load variations also needs to be considered since variations in load composition and consumption patterns can significantly change load model parameters and affect the performance of the adaptive wide-area controllers if not updated regularly. The change in load dynamics resulting from variations in load composition can impact the overall system dynamics, which manifests in the form of altered inter-area mode frequencies and oscillation intensity. This can be observed by performing Power Spectral Density (PSD) on generator velocity deviations [28], [31], [37].

Communication time delay is another aspect of wide-area measurement and control systems that must be considered. The performance of the proposed wide-area control method was evaluated against possible time delays by delaying PMU signals and observing the stability and robustness of the system for delays of up to 500 ms which is far beyond possible delays in modern wide-area measurement and control systems utilizing robust network designs.

A. CASE 1–25% DYNAMIC LOAD

In this case, the composite load model is customized to include 25% induction motor loads to add complex dynamics to the system. This technique is uniformly applied to all system loads by pairing various combinations of small and large induction motors to diversify the range of system dynamics. The adaptive wide-area SVC controllers are constructed by employing the MA load modeling technique, which relies on nonlinear Kalman filter estimates of equivalent area velocities, where for a third-order MA load model, the following SVC control expressions are obtained:

$$u_{3_k} = -0.0311\dot{\delta}_{3_k} + 0.1018\dot{\delta}_{3_{k+1}} - 0.1052\dot{\delta}_{3_{k+2}} + 0.0360\dot{\delta}_{3_{k+3}} \quad (22)$$

$$u_{4_k} = -0.0012\dot{\delta}_{4_k} + 0.0103\dot{\delta}_{4_{k+1}} - 0.0091\dot{\delta}_{4_{k+2}} + 0.0024\dot{\delta}_{4_{k+3}} \quad (23)$$

$$u_{5_k} = 0.0458\dot{\delta}_{5_k} - 0.1241\dot{\delta}_{5_{k+1}} + 0.1169\dot{\delta}_{5_{k+2}} - 0.0369\dot{\delta}_{5_{k+3}} \quad (24)$$

where k was chosen to be 0.001. The MA load model estimates resulted in 99.18%, 99.05% and 99.29% accuracy based on the RMSE criteria respectively. In order to evaluate the performance of the proposed controller, the system was simulated with a three-phase short-circuit fault applied on bus 308 in area 3, and the stability characteristics of the system were compared to the system with and without wide-area control. In the performed simulations, the Critical Clearing Time (CCT) of the system without wide-area control was chosen as the fault duration, which is often used as a criterion to benchmark first swing stability.

TABLE 1. Comparison of first swing stability (case 1).

Critical Clearing Time (CCT)		
No Wide-area Control	Wide-area Control (Without Load Dynamics)	Adaptive Wide-area Control (With Load Dynamics)
245 ms	321 ms	384 ms

In order to graphically show the results of the comparison, the generator rotor angles and frequency deviations in the Center of Inertia (COI) reference frame are shown in Figures 7 and 8, which compares the performance of the system in damping post-fault inter-area oscillations for each control scenario. The presented results clearly show the effectiveness and superior damping performance of the proposed adaptive wide-area control method, where load dynamics are considered.

The inclusion of load dynamics in the design of the proposed adaptive wide-area control method provides a more effective load modulation, which is observable from controlled susceptances, bus voltages and supplementary wide-area control signals of SVCs as illustrated in Figures 9 and 10. They provide a comparison between the performance and effectiveness of SVCs in all of the mentioned control scenarios. Correspondingly, as shown in Table 1, the proposed adaptive wide-area control method has improved the CCT of the system by 56.73%, while the wide-area controller without load dynamics has only managed to achieve 31.02% improvement. Based on the obtained results, it is clear that the proposed adaptive wide-area control method has significantly enhanced the SVCs ability to improve the stability of the system.

B. CASE 2–50% DYNAMIC LOAD

In this case, the composite load model was modified to increase the portion of induction motor loads to 50% in order to provide a uniform case. The following adaptive wide-area SVC control expressions were obtained after applying the MA load modeling technique:

$$u_{3_k} = -0.0821\dot{\delta}_{3_k} + 0.2695\dot{\delta}_{3_{k+1}} - 0.2824\dot{\delta}_{3_{k+2}} + 0.0973\dot{\delta}_{3_{k+3}} \quad (25)$$

$$u_{4_k} = -0.3397\dot{\delta}_{4_k} + 1.0258\dot{\delta}_{4_{k+1}} - 1.0258\dot{\delta}_{4_{k+2}} + 0.3392\dot{\delta}_{4_{k+3}} \quad (26)$$

$$u_{5_k} = 0.2160\dot{\delta}_{5_k} - 0.5991\dot{\delta}_{5_{k+1}} + 0.5624\dot{\delta}_{5_{k+2}} - 0.1770\dot{\delta}_{5_{k+3}} \quad (27)$$

The constant k value of 0.001 was used and the MA load model estimates produce 98.06%, 98.11% and 98.59% accuracy based on the RMSE criteria, respectively. The above SVC control expressions rely on estimations of aggregated

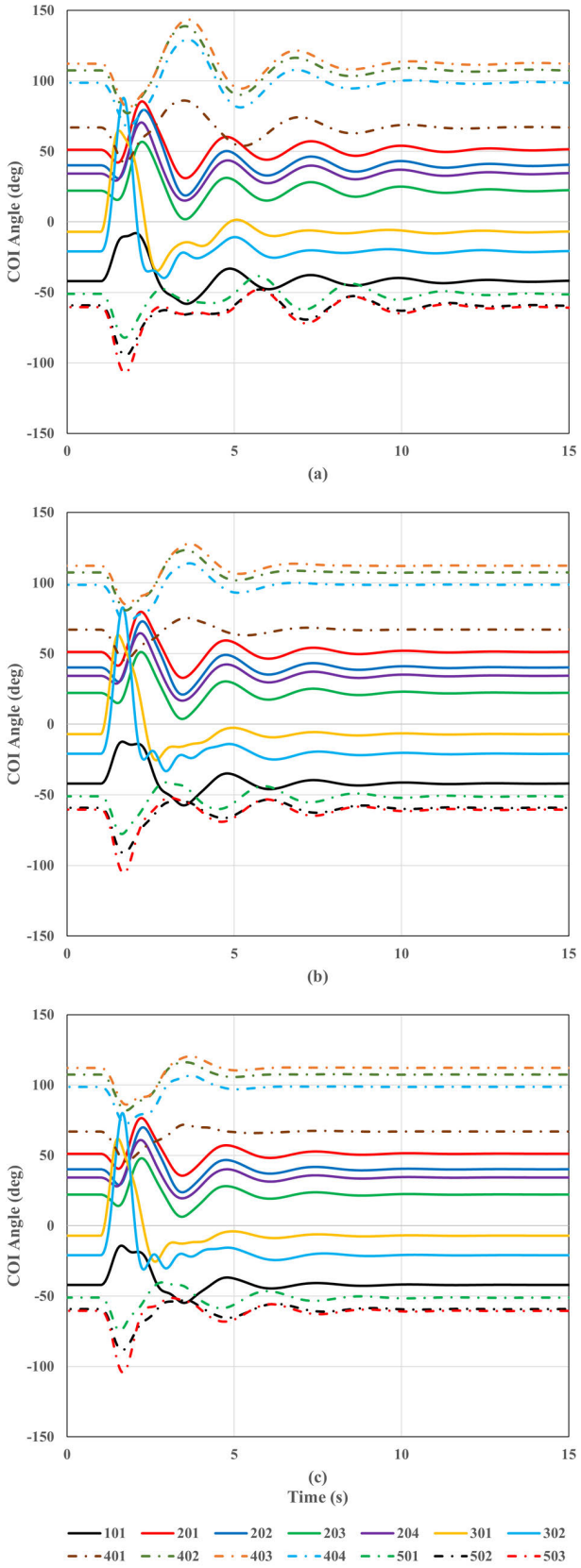

FIGURE 7. Generator rotor angles (Case 1) (a) without wide-area control, (b) with wide-area control and (c) with the proposed adaptive wide-area control method.

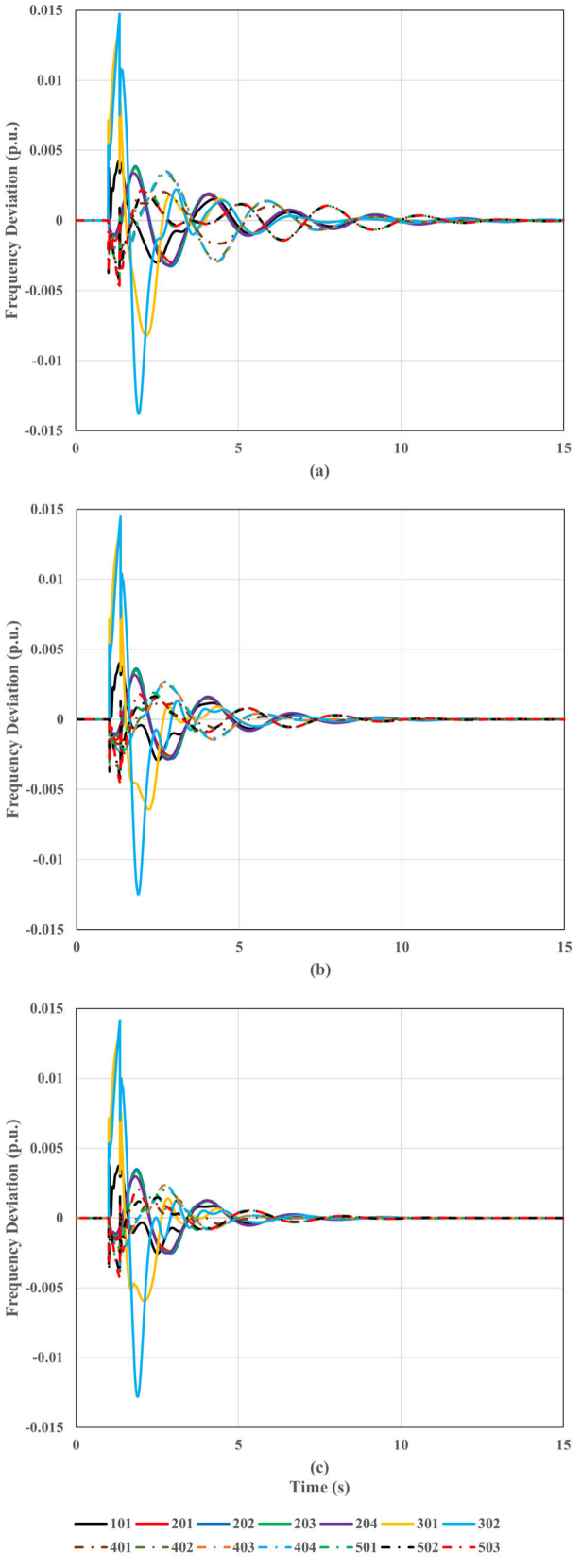

FIGURE 8. Frequency deviation at generator buses (Case 1) (a) without wide-area control, (b) with wide-area control and (c) with the proposed adaptive wide-area control method.

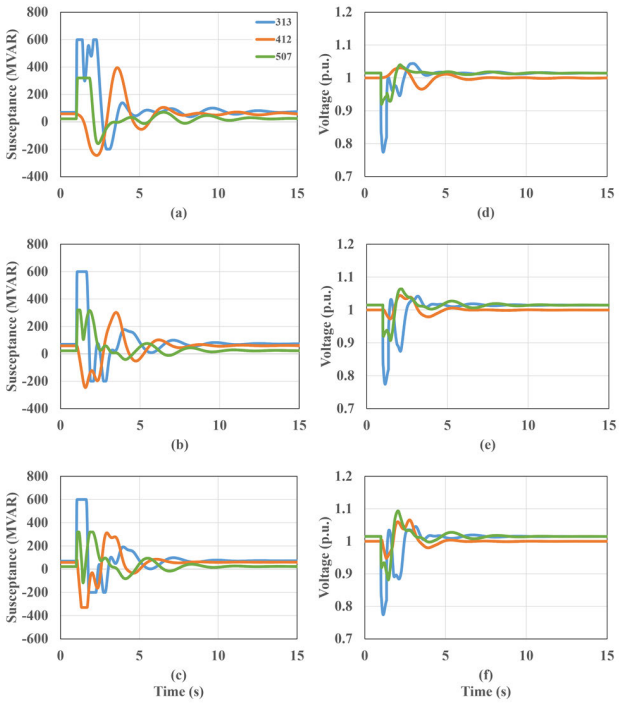

FIGURE 9. Susceptances of SVCs (a) without wide-area control, (b) with wide-area control (c) with the proposed adaptive wide-area control method; Terminal voltages of SVCs (d) without wide-area control, (e) with wide-area control (f) with the proposed adaptive wide-area control method (case 1).

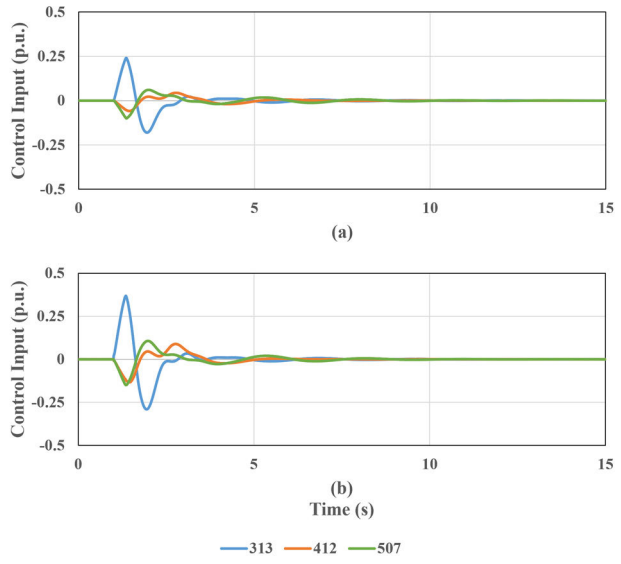

FIGURE 10. Comparison of supplementary control signals (Case 1) (a) wide-area control, (b) the proposed adaptive wide-area control method.

area velocities and predictions, which were obtained by applying the mentioned nonlinear Kalman filtering approach. Similar to the previous case, the performance of the proposed adaptive wide-area control method was assessed by applying a three-phase short-circuit fault on bus 308 in area 3.

TABLE 2. Comparison of first swing stability (case 2).

Critical Clearing Time (CCT)		
No Wide-area Control	Wide-area Control (Without Load Dynamics)	Adaptive Wide-area Control (With Load Dynamics)
85 ms	225 ms	292 ms

The stability characteristics of the system were then compared to the system without wide-area control and with the wide-area controller without the inclusion of load dynamics. Again, the CCT of the system without wide-area control was chosen as the fault duration to benchmark the stability of the system for each control scenario. The results of this comparison are shown in Figures 11, 12, 13 and 14, showing the generator rotor angles and frequency deviations in the COI reference frame, controlled SVC susceptances along with SVC bus voltages and supplementary SVC wide-area control signals. The results in Table 2 show that the proposed adaptive wide-area control method has improved the CCT of the system by 57.84%, while the wide-area controller without load dynamics has only managed to achieve a 21.62% improvement in increasing the CCT of the system. The presented results clearly show the effects of change in load composition achieved by an increase in the dynamic portion of the load, which has changed the oscillatory behavior of the post-fault system as a result of a large disturbance. However, despite the changes made in the load composition, the proposed adaptive wide-area control method has improved the damping of post-fault inter-area oscillations through a more effective SVC load modulation by adapting to load variations.

C. CASE 3 – 75% DYNAMIC LOAD

In this case, the dynamic portion of the load was increased by including 75% induction motor loads in the composite load model. By applying the MA load modeling technique, the following adaptive wide-area SVC control expressions are obtained:

$$u_{3_k} = 0.0018\dot{\delta}_{3_k} + 0.1868\dot{\delta}_{3_{k+1}} - 0.3391\dot{\delta}_{3_{k+2}} + 0.1553\dot{\delta}_{3_{k+3}} \quad (28)$$

$$u_{4_k} = -0.9755\dot{\delta}_{4_k} + 3.1693\dot{\delta}_{4_{k+1}} - 3.3543\dot{\delta}_{4_{k+2}} + 1.1678\dot{\delta}_{4_{k+3}} \quad (29)$$

$$u_{5_k} = 2.0220\dot{\delta}_{5_k} - 5.7755\dot{\delta}_{5_{k+1}} + 5.5263\dot{\delta}_{5_{k+2}} - 1.7685\dot{\delta}_{5_{k+3}} \quad (30)$$

where the constant k value of 0.001 is chosen and the MA load model estimates yield 95.66%, 96.24% and 96.13% accuracy based on the RMSE criteria, respectively. Again, the above SVC control expressions rely on applying the mentioned nonlinear Kalman filtering approach to estimate and predict aggregated area velocities.

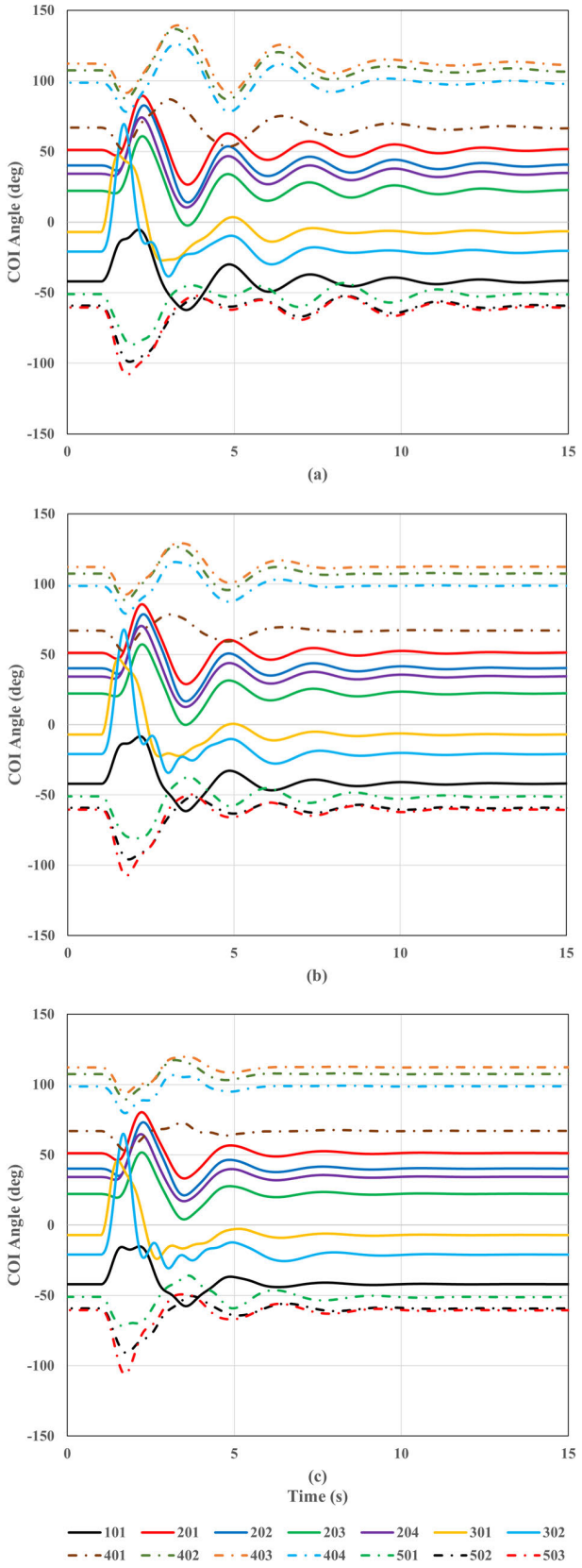

FIGURE 11. Generator rotor angles (case 2) (a) without wide-area control, (b) with wide-area control and (c) with the proposed adaptive wide-area control method.

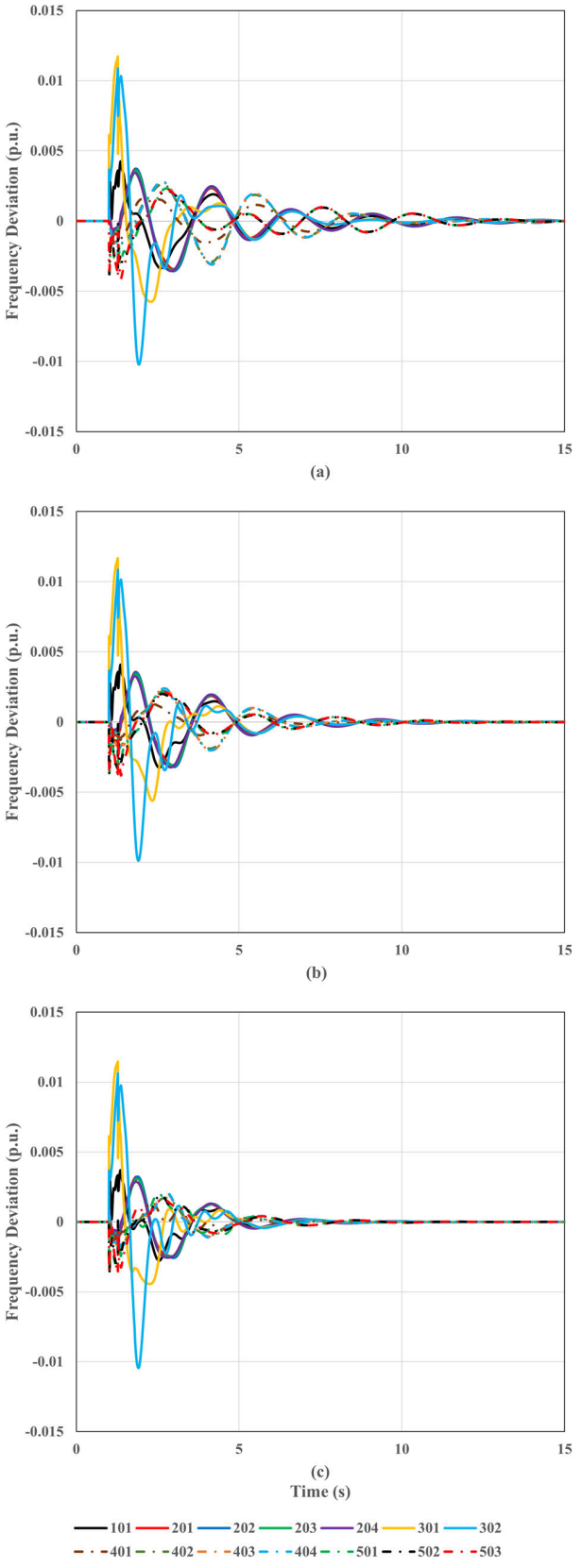

FIGURE 12. Frequency deviation at generator buses (case 2) (a) without wide-area control, (b) with wide-area control and (c) with the proposed adaptive wide-area control method.

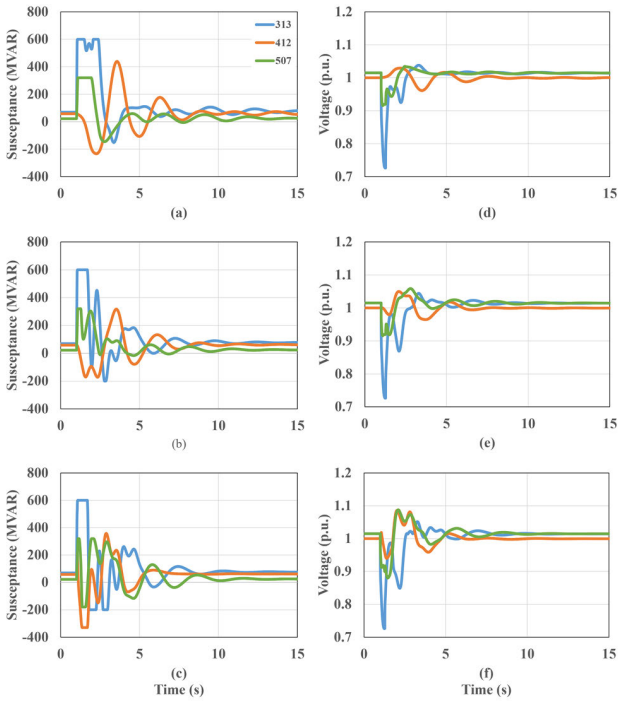

FIGURE 13. Susceptances of SVCs (a) without wide-area control, (b) with wide-area control (c) with the proposed adaptive wide-area control method; Terminal voltages of SVCs (d) without wide-area control, (e) with wide-area control (f) with the proposed adaptive wide-area control method (case 2).

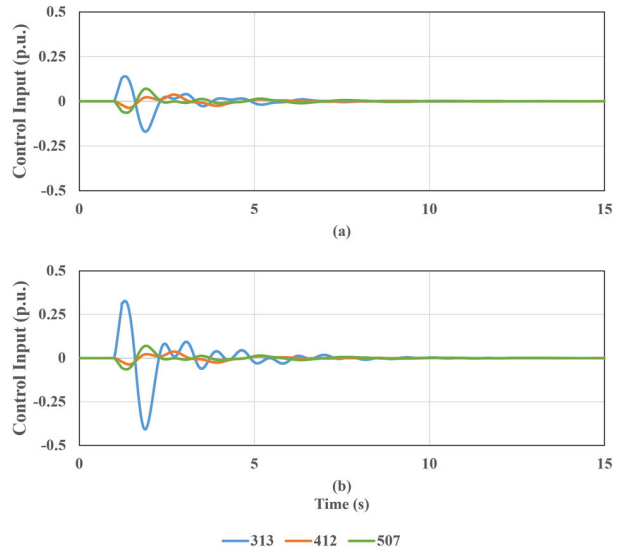

FIGURE 14. Comparison of supplementary control signals (case 2) (a) wide-area control, (b) the proposed adaptive wide-area control.

The system was simulated with the same fault scenario as previous cases, and the performance of the proposed adaptive wide-area control method was compared against the system without wide-area control and with wide-area control without accounting for load dynamics in controller design. Comparisons of the post-fault trajectory of the generator rotor angles and bus frequency deviations in the COI reference frame are shown in Figures 15 and 16. The SVC susceptances, bus voltages and supplementary wide-area control signals are represented in Figures 17 and 18, demonstrating the performance of load modulating SVCs in all three control scenarios.

In comparison to previous cases, as depicted in Table 3, the CCT of the system has been substantially reduced, which is due to the heavy component of induction motors used in the composite load model. However, the proposed adaptive wide-area control method has managed to improve the CCT of the system by 40.21%, while the wide-area controller without load dynamics has only improved the CCT by 10.87%. The obtained results clearly show the effectiveness and superior performance of the proposed adaptive wide-area control method in both post-fault oscillation damping and CCT improvements. Additionally, the proposed adaptive wide-area control algorithm has even managed to improve the first swing stability of the system by substantially increasing and saturating SVC inductive and capacitive limits as shown in Figure 17 (C), following a large disturbance which typically requires a different control action.

D. EFFECT OF LOAD COMPOSITION ON OSCILLATORY MODES

Load composition can play an important role in the determination of power system dynamics. In power system stability studies, the composition and consumption pattern of loads can significantly affect the frequency and intensity of oscillatory generator behavior [28]. This effect can be observed through spectrum analysis of generator velocity deviations, which can extract frequencies and intensities of oscillatory modes [31]. In order to observe the effects of load composition variations on the test system, PSD analysis was applied to generator velocity deviations for all of the presented cases. The results of the PSD analysis are shown in Figure 19. The obtained results clearly show that the pattern of oscillations in terms of frequency and intensity has drastically changed for all system modes as a result of variations in the load composition, which was achieved by changing the ratio of dynamic and static loads in the form of induction motor and constant impedance loads. It can be concluded that the system's dynamic behavior has changed substantially by the inclusion of different amounts of induction motor loads in the load composition. It is important to mention that the use of constant impedance loads in dynamic stability studies often leads to overly optimistic outcomes, which undermine the dynamic characteristics of loads and their adverse effects on overall system dynamics. Therefore, in dynamic stability studies, it is essential to include loads with complex dynamic characteristics in order to represent a more realistic scenario.

E. EFFECT OF COMMUNICATION DELAY ON PERFORMANCE

Communication time delay is an important issue in the design and implementation of wide-area measurement and control systems. This time delay can adversely affect the performance

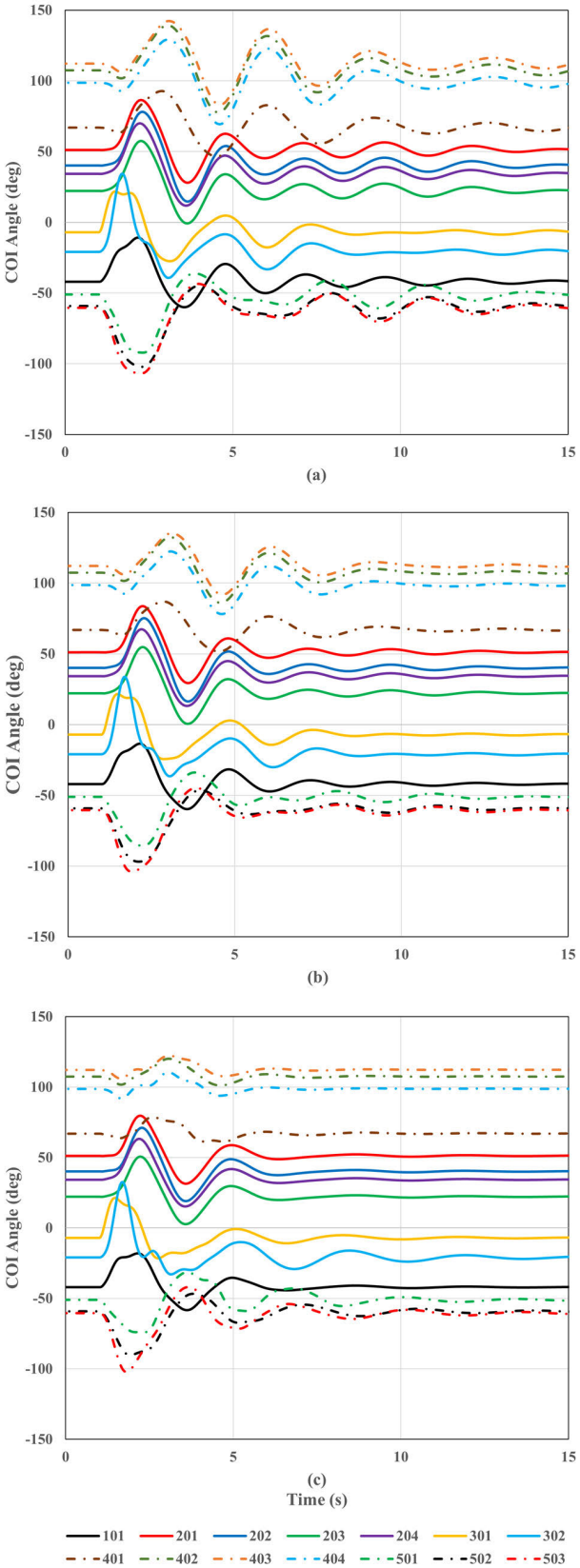

FIGURE 15. Generator rotor angles (case 3) (a) without wide-area control, (b) with wide-area control and (c) with the proposed adaptive wide-area control method.

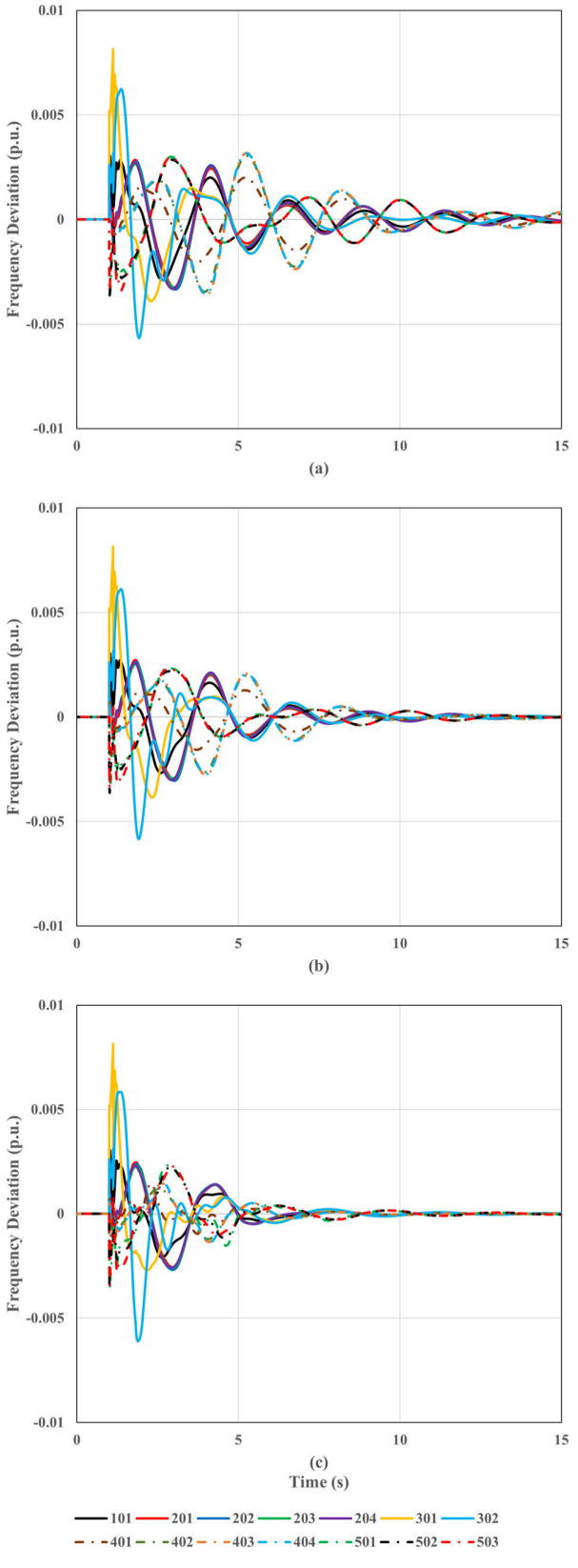

FIGURE 16. Frequency deviation at generator buses (case 3) (a) without wide-area control, (b) with wide-area control and (c) with the proposed adaptive wide-area control method.

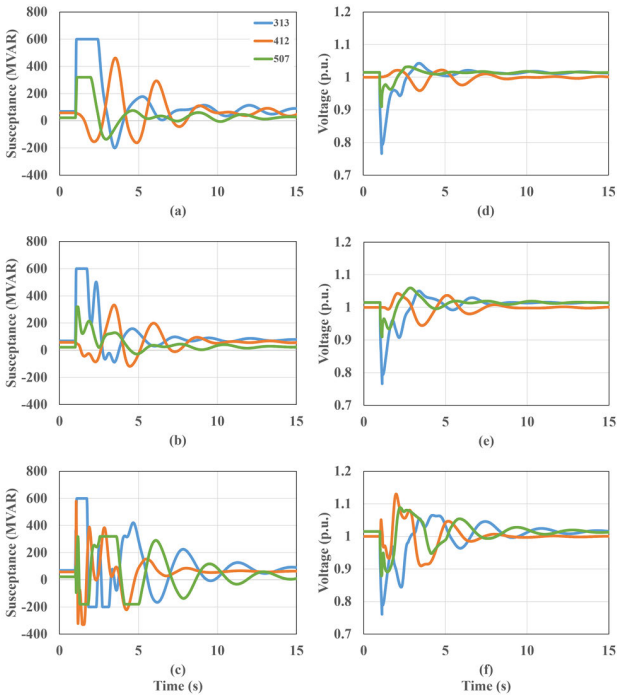

FIGURE 17. Susceptances of SVCs (a) without wide-area control, (b) with wide-area control (c) with the proposed adaptive wide-area control method; Terminal voltages of SVCs (d) without wide-area control, (e) with wide-area control (f) with the proposed adaptive wide-area control method (case 3).

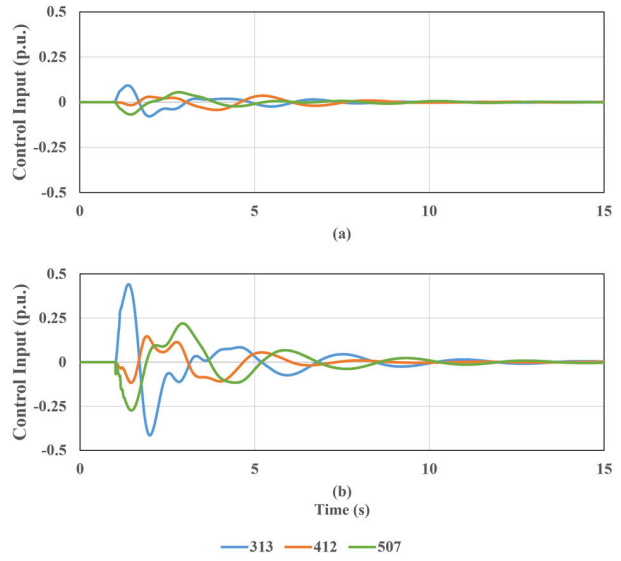

FIGURE 18. Comparison of supplementary control signals (case 3) (a) wide-area control, (b) the proposed adaptive wide-area control.

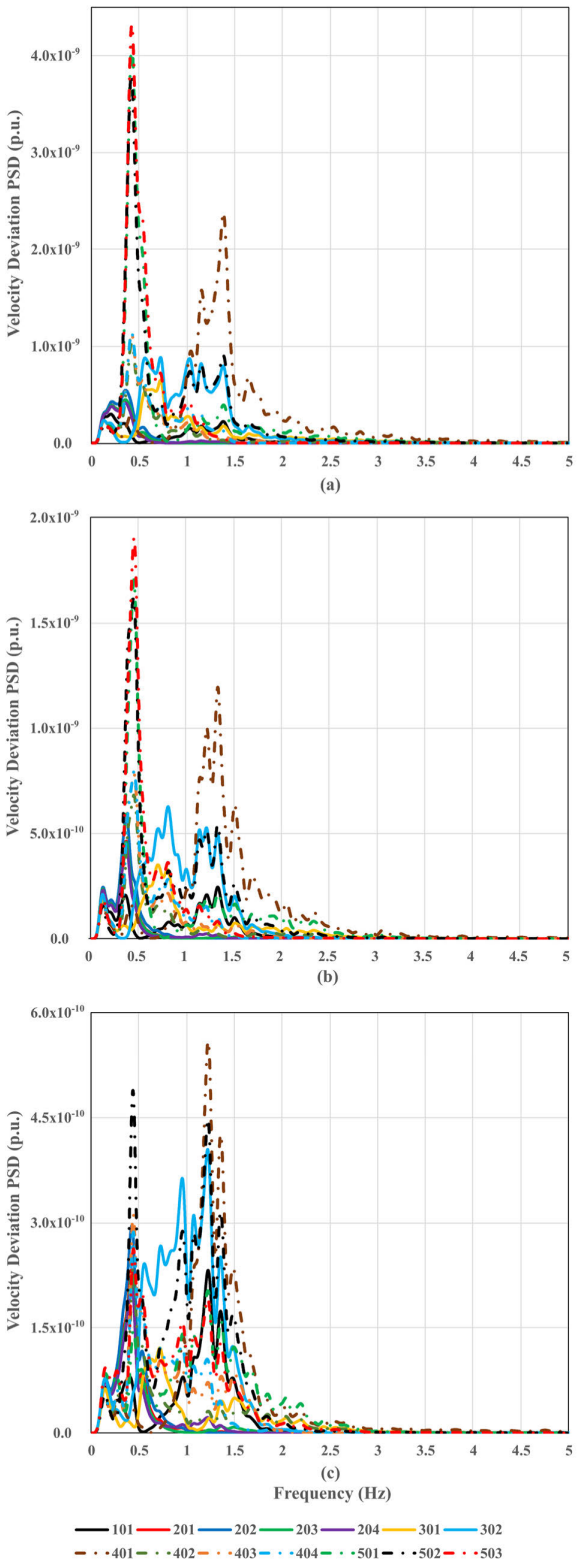

FIGURE 19. Power Spectral Density (PSD) of generator velocity deviations (a) 25% dynamic load (case 1) (b) 50% dynamic load (case 2) (c) 75% dynamic load (case 3).

of wide-area measurement and control systems and reduce their effectiveness. The performance of wide-area measurement and control systems depends on timely measurements of system states provided by measurement devices such as PMUs and associated communication network infrastructure. Like all communication networks, wide-area measurement and control systems can suffer from signal latency and time delay issues, often resolved by a robust network design and

TABLE 3. Comparison of first swing stability (case 3).

Critical Clearing Time (CCT)		
No Wide-area Control	Wide-area Control (Without Load Dynamics)	Adaptive Wide-area Control (With Load Dynamics)
92 ms	102 ms	129 ms

TABLE 4. Induction Motor combination for composite load.

Bus	Small Induction Motor	Large Induction Motor
102	5.5 kW	15 kW
205	22 kW	185 kW
206	30 kW	132 kW
207	18.5 kW	315 kW
208	15 kW	90 kW
211	5.5 kW	11 kW
212	37 kW	200 kW
215	15 kW	185 kW
216	7.5 kW	45 kW
217	11 kW	55 kW
306	18.5 kW	315 kW
307	18.5 kW	315 kW
308	37 kW	200 kW
309	22 kW	185 kW
312	15 kW	90 kW
313	30 kW	132 kW
314	5.5 kW	395 kW
405	37 kW	200 kW
406	5.5 kW	395 kW
408	22 kW	90 kW
409	30 kW	132 kW
410	7.5 kW	45 kW
411	11 kW	55 kW
412	15 kW	90 kW
504	37 kW	200 kW
507	5.5 kW	11 kW
508	5.5 kW	395 kW
509	15 kW	90 kW

implementation. Nowadays, robust network design strategies and data transfer and management techniques are employed to enhance the performance of wide-area monitoring and control systems which has improved the quality of data obtained by PMUs located at remote locations of power systems which are often susceptible to time delay issues. However, despite all enhancements, robust design and implementation strategies, it is essential to account for the effects of time delay in all wide-area monitoring and control system designs and applications to evaluate the performance and effectiveness of implementations.

Typically, the communication time delay in a robust wide-area measurement and control system with a high bandwidth

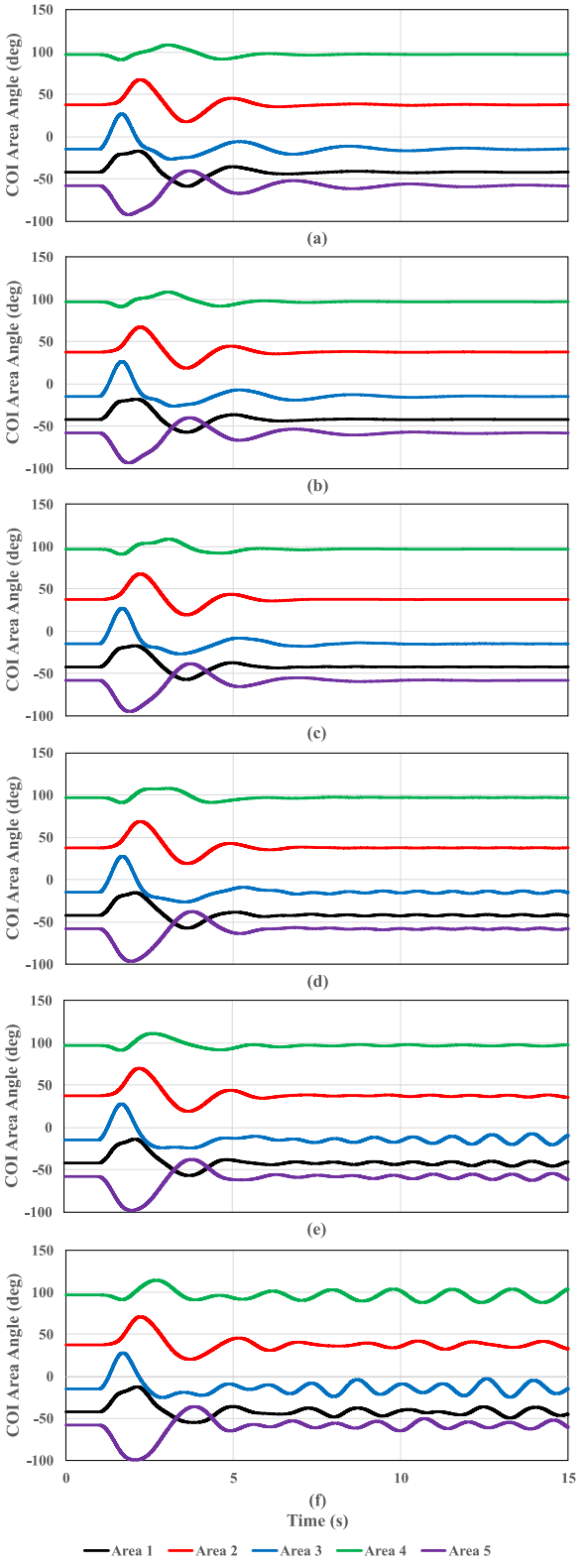

FIGURE 20. COI area angles (a) No time delay (b) 100 ms delay (c) 200 ms delay (d) 300 ms delay (e) 400 ms delay (f) 500 ms delay.

network is small and does not impose any performance degradation issues [21], [38]. For performance evaluation and preservation of consistency with the work presented in [21],

TABLE 5. Induction motor parameters for composite load.

Machine Rating			All induction motors are 415 V / 50 Hz machines										
Apparent Power (KVA)	Power (KW)	Speed (RPM)	No Poles	T_B (Nm) (Base Torque)	I_B (A) (Base Current)	T_{lr} (Nm) (Locked Rotor Torque)	I_{lr} (A) (Locked Rotor Current)	Rs (Ohms)	Lls (mH)	Lm (mH)	R'r (Ohms)	L'lr (mH)	J (Kg.m^2)
7.090	5.5	2940	2	39.279	9.912	11.289	27.295	1.66267	0.77320	176.96846	0.88528	30.89292	0.00980
9.854	7.5	2940	2	54.593	13.776	24.339	45.235	1.04982	0.55632	156.62305	0.83106	35.88311	0.01953
14.548	11	1465	4	161.189	20.337	27.943	62.165	0.64524	0.37683	57.64002	0.26737	14.63026	0.06837
18.755	15	2945	2	103.901	26.218	19.415	66.305	0.41565	0.29230	73.70030	0.30282	13.04115	0.04908
23.918	18.5	1460	4	265.006	33.435	21.890	50.415	0.39826	0.22921	71.64836	0.33077	18.71884	0.13234
28.624	22	1470	4	317.148	40.014	166.558	166.886	0.33523	0.19152	40.72771	0.17653	4.60344	0.18624
38.925	30	1475	4	431.291	54.415	251.790	275.739	0.20297	0.14084	29.65402	0.09400	2.71512	0.28513
44.416	37	2950	2	246.062	62.090	233.835	424.038	0.16612	0.12343	32.54080	0.07367	1.59795	0.17701
57.575	45	1480	4	637.933	80.487	241.176	374.717	0.11242	0.09522	21.29249	0.04979	2.07367	0.41442
67.604	55	1480	4	749.053	94.507	300.856	454.120	0.09030	0.08109	20.22573	0.04289	1.68657	0.71029
108.669	90	1483	4	1204.054	151.914	416.374	754.952	0.05114	0.05045	13.58885	0.02146	1.00966	1.48313
158.376	132	1487	4	1754.806	221.401	538.039	1211.605	0.03181	0.03461	9.40203	0.01064	0.62277	2.57738
227.176	185	1485	4	2517.109	317.579	578.119	1355.529	0.02832	0.02413	6.45651	0.00917	0.57664	3.83130
238.976	200	1486	4	2647.845	334.074	815.099	1761.054	0.01814	0.02294	6.33961	0.00770	0.43251	3.46756
380.747	315	1490	4	4218.663	532.262	983.053	2878.083	0.01227	0.01440	3.74389	0.00344	0.26488	10.43993
469.047	395	1489	4	5197.029	655.701	1375.157	3623.247	0.00794	0.01169	3.21616	0.00306	0.20994	9.92618

the same time delay of 40 ms was imposed on all PMU signals, which is larger than the expected time delay in a realistic system. The added time delay did not result in any performance degradation in any of the presented load cases, and the same CCT values as in Tables 1, 2 and 3 and post-fault trajectories as shown in Figures 7 to 18 were observed, which shows the robustness of the proposed wide-area control method to possible communication time delays.

While the communication time delay in a realistic system is not expected to be larger than the simulated value, in order to account for more extreme scenarios, the time delay imposed on PMU signals were increased and delays of up to 200 ms resulted in CCT values and post-fault trajectories similar to the no-delay system. However, time delays larger than 200 ms resulted in the loss of performance, and in extreme cases beyond 200 ms, instability was observed. For the purpose of demonstration, aggregated area angles in COI reference frame for case 3 with the highest component of dynamic loads for time delays of up to 500 ms are shown in Figure 20, which shows the response of the proposed wide-area control method to post-fault inter-area oscillations for a wide range of time delays. It can be concluded that the proposed wide-area control method is effective and robust to a wide range of expected communication time delays associated with wide-area measurement and control systems and provides stability improvement through damping of post-fault inter-area oscillations.

VI. CONCLUSION

In this paper, an energy function-based adaptive wide-area control method is presented. The proposed method is a kinetic energy-based control strategy that provides damping of post-fault inter-area oscillations based on inter-area dynamics obtained through PMU measurements and a non-linear Kalman filtering approach. The proposed wide-area control strategy modulates the area loads by incorporating load dynamics in the controller design and formulation and can adapt to load changes and variations. The load dynamics are modeled as a moving average (MA) process estimated based on load dynamics data obtained through PMU measurements. The proposed wide-area control method is applied to load modulating SVCs and enhances their load modulating capability resulting in better post-fault oscillation damping and improving overall system stability and performance. The proposed method was evaluated on the simplified 14 generator model of the Southeast Australian power system by employing a composite load model with varying combinations of induction motor loads of different sizes and ratings to add a range of complex and diverse dynamics. The performance of the proposed method was compared to the system without wide-area control and with wide-area control without accounting for load dynamics in control design. The results show the superiority of the proposed adaptive wide-area control method in terms of damping post-fault inter-area oscillations and CCT improvements for presented loading conditions. In the future, to further expand and develop the proposed wide-area control approach, other power and energy storage devices such as Battery Energy Storage Systems (BESS), Superconducting Magnetic (SMES) and Capacitive (CES) Energy Storage systems can be considered. Also, BESS systems in the distribution level networks can be used through clustering and networked-based multi-agent cooperative control methods and consensus-based control algorithms, making them a viable distributed energy source for damping and stability improvement applications.

REFERENCES

[1] M. Klein, G. J. Rogers, and P. Kundur, "A fundamental study of inter-area oscillations in power systems," *IEEE Trans. Power Syst.*, vol. 6, no. 3, pp. 914–921, Aug. 1991.

[2] P. Kundur, *Power System Stability and Control*. Noida, India: McGraw-Hill, 1994, p. 1176.

[3] M. H. Haque, "Application of energy function to assess the first-swing stability of a power system with a SVC," *IEE Proc., Gener., Transmiss. Distrib.*, vol. 152, no. 6, pp. 806–812, 2005.

[4] H. Ghasemi, C. Canizares, and A. Moshref, "Oscillatory stability limit prediction using stochastic subspace identification," *IEEE Trans. Power Syst.*, vol. 21, no. 2, pp. 736–745, May 2006.

[5] Z. Qihua and J. Jin, "Robust SVC controller design for improving power system damping," *IEEE Trans. Power Syst.*, vol. 10, no. 4, pp. 1927–1932, Nov. 1995.

[6] E. N. Lerch, D. Povh, and L. Xu, "Advanced SVC control for damping power system oscillations," *IEEE Trans. Power Syst.*, vol. 6, no. 2, pp. 524–535, May 1991.

[7] M. Ghandhari, G. Andersson, and I. A. Hiskens, "Control Lyapunov functions for controllable series devices," *IEEE Trans. Power Syst.*, vol. 16, no. 4, pp. 689–694, Nov. 2001.

[8] M. E. Aboul-Ela, A. A. Sallam, J. D. McCalley, and A. A. Fouad, "Damping controller design for power system oscillations using global signals," *IEEE Trans. Power Syst.*, vol. 11, no. 2, pp. 767–773, May 1996.

[9] M. R. Younis and R. Iravani, "Wide-area damping control for inter-area oscillations: A comprehensive review," in *Proc. IEEE Electr. Power Energy Conf.*, Aug. 2013, pp. 1–6.

[10] V. Salehi, A. Mazloomzadeh, and O. Mohammed, "Development and implementation of a phasor measurement unit for real-time monitoring, control and protection of power systems," in *Proc. IEEE Power Energy Soc. Gen. Meeting*, Jul. 2011, pp. 1–7.

[11] M. Zima, M. Larsson, P. Korba, C. Rehtanz, and G. Andersson, "Design aspects for wide-area monitoring and control systems," *Proc. IEEE*, vol. 93, no. 5, pp. 980–996, May 2005.

[12] N. R. Chaudhuri, A. Domahidi, R. Majumder, B. Chaudhuri, P. Korba, S. Ray, and K. Uhlen, "Wide-area power oscillation damping control in Nordic equivalent system," *IET Gener., Transmiss. Distrib.*, vol. 4, no. 10, pp. 1139–1150, 2010.

[13] M. Zarghami, M. L. Crow, and S. Jagannathan, "Nonlinear control of FACTS controllers for damping interarea oscillations in power systems," *IEEE Trans. Power Del.*, vol. 25, no. 4, pp. 3113–3121, Oct. 2010.

[14] Y. Li, C. Rehtanz, S. Ruberg, L. Luo, and Y. Cao, "Wide-area robust coordination approach of HVDC and FACTS controllers for damping multiple interarea oscillations," *IEEE Trans. Power Del.*, vol. 27, no. 3, pp. 1096–1105, Jul. 2012.

[15] F. R. Segundo, J. Dobrowolski, H. Nussbaumer, P. Korba, and E. Barocio, "State-feedback control for damping inter-area oscillations on electrical power systems," in *Proc. IEEE Int. Autumn Meeting Power, Electron. Comput. (ROPEC)*, Nov. 2018, pp. 1–6.

[16] M. Elsisi, M. Soliman, M. A. S. Aboelela, and W. Mansour, "GSA-based design of dual proportional integral load frequency controllers for nonlinear hydrothermal power system," *World Acad. Sci., Eng. Technol.*, vol. 9, pp. 1142–1148, Sep. 2015.

[17] M. Elsisi, M. Soliman, M. A. S. Aboelela, and W. Mansour, "Improving the grid frequency by optimal design of model predictive control with energy storage devices," *Optim. Control Appl. Methods*, vol. 39, no. 1, pp. 263–280, Jan. 2018.

[18] J. Machowski and D. Nelles, "Power system transient stability enhancement by optimal control of static VAR compensators," *Int. J. Electr. Power Energy Syst.*, vol. 14, no. 6, pp. 411–421, Dec. 1992.

[19] J. Machowski and D. Nelles, "A static VAR compensator control strategy to maximize power system damping," *Electr. Mach. Power Syst.*, vol. 24, no. 5, pp. 477–495, Jul. 1996.

[20] J. Machowski, P. Kacejko, Ł. Nogal, and M. Wancerz, "Power system stability enhancement by WAMS-based supplementary control of multi-terminal HVDC networks," *Control Eng. Pract.*, vol. 21, no. 5, pp. 583–592, May 2013.

[21] A. Vahidnia, G. Ledwich, and E. W. Palmer, "Transient stability improvement through wide-area controlled SVCs," *IEEE Trans. Power Syst.*, vol. 31, no. 4, pp. 3082–3089, Jul. 2016.

[22] E. Palmer, G. Ledwich, and A. Vahidnia, "Delay compensation in the wide area control of SVCs for first swing stabilisation and damping," in *Proc. Australas. Univ. Power Eng. Conf. (AUPEC)*, Sep. 2016, pp. 1–5.

[23] A. Vahidnia, L. Meegahapola, G. Ledwich, and R. Memisevic, "Application of wide-area controls in Australian power system," in *Proc. IEEE PES Innov. Smart Grid Technol. Conf. Eur. (ISGT-Europe)*, Sep. 2017, pp. 1–6.

[24] P. W. Sauer and M. A. Pai, *Power System Dynamics and Stability*. Upper Saddle River, NJ, USA: Prentice-Hall, 1998.

[25] A. Fouad and S. Stanton, "Transient stability of a multi-machine power system. Part I: Investigation of system trajectories," *IEEE Trans. Power App. Syst.*, vol. PAS-100, no. 7, pp. 3408–3416, Jul. 1981.

[26] A. Vahidnia, G. Ledwich, E. Palmer, and A. Ghosh, "Wide-area control through aggregation of power systems," *IET Gener., Transmiss. Distrib.*, vol. 9, no. 12, pp. 1292–1300, Sep. 2015.

[27] E. Palmer and G. Ledwich, "Switching control for power systems with line losses," *IEE Proc., Gener., Transmiss. Distrib.*, vol. 146, no. 5, pp. 435–440, 1999.

[28] A. Sharafi, A. Vahidnia, and M. Jalili, "Measurement-based identification of system load models for low-frequency dynamics," in *Proc. 9th Int. Conf. Power Energy Syst. (ICPES)*, Dec. 2019, pp. 1–6.

[29] A. Vahidnia, G. Ledwich, E. Palmer, and A. Ghosh, "Dynamic equivalent state estimation for multi-area power systems with synchronized phasor measurement units," *Electr. Power Syst. Res.*, vol. 96, pp. 170–176, Mar. 2013.

[30] A. Vahidnia, G. Ledwich, E. Palmer, and A. Ghosh, "Identification and estimation of equivalent area parameters using synchronised phasor measurements," *IET Gener., Transmiss. Distrib.*, vol. 8, no. 4, pp. 697–704, 2014.

[31] A. Vahidnia, G. Ledwich, E. Palmer, and A. Ghosh, "Generator coherency and area detection in large power systems," *IET Gener., Transmiss. Distrib.*, vol. 6, no. 9, pp. 874–883, Sep. 2012.

[32] IEEE Committee, "Load representation for dynamic performance analysis (of power systems)," *IEEE Trans. Power Syst.*, vol. 8, no. 2, pp. 472–482, May 1993.

[33] W. Price, C. W. Taylor, and G. J. Rogers, "Standard load models for power flow and dynamic performance simulation," *IEEE Trans. Power Syst.*, vol. 10, no. 3, pp. 1302–1313, Aug. 1995.

[34] E. O. Kontis, T. A. Papadopoulos, A. I. Chrysochos, and G. K. Papagiannis, "Measurement-based dynamic load modeling using the vector fitting technique," *IEEE Trans. Power Syst.*, vol. 33, no. 1, pp. 338–351, Jan. 2018.

[35] E. O. Kontis, A. I. Chrysochos, G. K. Papagiannis, and T. A. Papadopoulos, "Modeling of nonlinear dynamic power system loads using the vector fitting technique," in *Proc. 51st Int. Univ. Power Eng. Conf. (UPEC)*, Sep. 2016, pp. 1–6.

[36] M. Gibbard and D. Vowles, "Simplified 14-generator model of the south east Australian power system," School Elect. Electron. Eng., Power Syst. Dyn. Group, Revision 4, Univ. Adelaide, Adelaide, SA, Australia, Tech. Rep., 2014. [Online]. Available: https://www.researchgate.net/profile/Dj-Vowles-2/post/Can_anyone_help_me_with_dynamic_data_of_an_electrical_power_system_IEEE_test_system_or_other/attachment/59d62bc2c49f478072e9da76/AS%3A273536776638464%401442227657404/download/Simplified_14-Gen_System_Rev4_20140227_PSDGReportVersion.pdf

[37] C. Concordia and S. Ihara, "Load representation in power system stability studies," *IEEE Trans. Power App. Syst.*, vol. PAS-101, no. 4, pp. 969–977, Apr. 1982.

[38] M. Chenine and L. Nordstrom, "Modeling and simulation of wide-area communication for centralized PMU-based applications," *IEEE Trans. Power Del.*, vol. 26, no. 3, pp. 1372–1380, Jul. 2011.

AMIN SHARAFI (Graduate Student Member, IEEE) received the B.Eng. and M.Eng. degrees in electrical engineering from RMIT University, Melbourne, VIC, Australia, in 2012 and 2016, respectively, where he is currently pursuing the Ph.D. degree. His research interests include power systems, power electronics, control systems, system identification, and optimization problems.

ARASH VAHIDNIA (Senior Member, IEEE) received the Ph.D. degree in power engineering from the Queensland University of Technology (QUT). He is currently a Lecturer with the School of Engineering, RMIT University. He was a Research Fellow within the Power Engineering Group, QUT, before joining RMIT. He also has several years of industry experience working at power consultancy and utility firms. His research interests include power system stability, reliability, microgrids, renewable energies, and system planning and control.

MAHDI JALILI (Senior Member, IEEE) received the B.S. degree in electrical engineering from Tehran Polytechnic, Tehran, Iran, in 2001, the M.S. degree in electrical engineering from the University of Tehran, Tehran, in 2004, and the Ph.D. degree in synchronization in dynamical networks from the Swiss Federal Institute of Technology Lausanne, Lausanne, Switzerland. Then, he joined the Sharif University of Technology as an Assistant Professor. He is currently a Senior Lecturer with the School of Engineering, RMIT University, Melbourne, VIC, Australia. His research interests include network science, dynamical systems, social networks analysis and mining, and data analytics. He was a recipient of the Australian Research Council DECRA Fellowship and the RMIT Vice-Chancellor Research Fellowship. He is an Associate Editor of the IEEE CANADIAN JOURNAL OF ELECTRICAL AND COMPUTER ENGINEERING and an Editorial Board Member of the *Mathematical Problems in Engineering* and *Complex Adaptive Systems Modeling*.

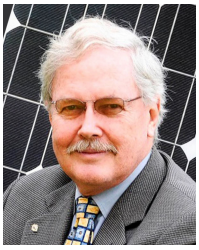

GERARD LEDWICH (Life Fellow, IEEE) received the Ph.D. degree in electrical engineering from The University of Newcastle, Newcastle, NSW, Australia, in 1976. He is currently a Research Professor of electric power with the School of Electrical Engineering and Robotics, Queensland University of Technology, Brisbane, QLD, Australia. He has 215 journal publications and 323 refereed conference publications. He has a Scopus H-index of 44 and a citation count of 8633. He has been involved in securing grants of more than AU$16 million with the majority of them were in explicit partnership with industry. His research interests include power systems, power electronics, and wide area control of smart grid.